1-2014

Analysis of a Chemical Model System Leading to Chiral Symmetry Breaking: Implications for the Evolution of Homochirality

Brandy N. Morneau
University of New Haven, BMorneau@newhaven.edu

Jaclyn M. Kubala

Carl Barratt
University of New Haven, CBarratt@newhaven.edu

Pauline Schwartz
University of New Haven, PSchwartz@newhaven.edu

Publisher Citation

Morneau, B., Kubala, J., Barratt, C., & Schwart, P. (2014). Analysis of a chemical model system leading to chiral symmetry breaking: implications for the evolution of homochirality. Journal of Mathematical Chemistry, 52(1), 268-282. doi: 10.1007/s10910-013-0261-5

Comments

This is the authors' accepted version of an article that was published in Journal of Mathematical Chemistry. The final publication is available at Springer via http://dx.doi.org/10.1007/s10910-013-0261-5 (published online Sept. 26, 2013)

Final Manuscript of an article appearing in J. Math. Chem. 52:268-282, 2014. See cover page.

Analysis of a chemical model system leading to chiral symmetry breaking: Implications for the evolution of homochirality

Brandy N. Morneau[a], Jaclyn M. Kubala[a], Carl Barratt[b] and Pauline M. Schwartz[*a]

[a] Department of Chemistry and Chemical Engineering, Tagliatela College of Engineering, University of New Haven, West Haven, CT, 06516, USA

[b] Department of Mechanical, Civil and Environmental Engineering, Tagliatela College of Engineering, University of New Haven, West Haven, CT, 06516, USA

*Corresponding author: Tel.: 203-932-7170; fax: 203-931-6077

E-mail: pschwartz@newhaven.edu

Abstract

Explaining the evolution of a predominantly homochiral environment on the early Earth remains an outstanding challenge in chemistry. We explore here the mathematical features of a simple chemical model system that simulates chiral symmetry breaking and amplification towards homochirality. The model simulates the reaction of a prochiral molecule to yield enantiomers via interaction with an achiral surface. Kinetically, the reactions and rate constants are chosen so as to treat the two enantiomeric forms symmetrically. The system, however, incorporates a mechanism whereby a random event might trigger chiral symmetry breaking and the formation of a dominant enantiomer; the non-linear dynamics of the chemical system are such that small perturbations may be amplified to near homochirality. Mathematical analysis of the behavior of the chemical system is verified by both deterministic and stochastic numerical simulations. Kinetic description of the model system will facilitate exploration of experimental validation. Our model system also supports the notion that one dominant enantiomeric structure might be a template for other critical molecules.

Keywords: Bifurcation Deterministic kinetics Lyapunov stability Non-linear Quasi-equilibrium Symmetry breaking

1. Introduction

The emergence and amplification of chirality remain as an outstanding problem in understanding prebiotic chemistry [1-3]. The fact that, on Earth, living systems are composed predominantly of L-amino acids and D-sugars is in stark contrast with the observation that simple chemical synthesis of these molecules from achiral precursors results in racemic mixtures of enantiomers, giving both R- and S-configurations in equal proportions. Indeed, in a biological environment, the chirality of monomers is critical to the effective functioning of macromolecules. Amino acids and sugars, the respective precursors for proteins and nucleic acids, must exhibit one chiral form; otherwise, the folding and shape of biological polymers like proteins, RNA, and DNA would not result in proper function. It is thus reasonable to assume that the chemical evolution of homochirality of critical biological molecules is an essential, early event for the advancement of life throughout the universe [1-4].

There are many theories of how a predominately chiral environment may have evolved that have been inspired by experimental observations and hypothetical systems. In his 1953 seminal paper, F.C. Frank proposed a model in which each of the two enantiomers of an asymmetric molecule is catalytic for its own synthesis and is inhibitory for the production of the other enantiomer; as a result the autocatalytic reaction amplifies any initial enantiomer imbalance [5]. Frank's model includes several important features that lead to chiral symmetry breaking, including the open and non-equilibrium nature of the system, the cross-inhibition, and the autocatalytic production of the chiral species [5-7]. Investigation of the dynamic aspects of such chemical model systems is important in understanding chiral symmetry breaking [8-13]. In other cases, authors sought to produce simpler models that operate under fewer assumptions. For example, the "toy" model proposed by Saito and Hyuga describe closed rather than open systems and included no cross-inhibition, while demonstrating varying strengths of autocatalysis and recycling [14]. Other important model systems have incorporated polymerization and/or epimerization steps in the chemical mechanism [15, 16]. These models focus on the formation of hetero- and homo-dimers. Chemical model systems such as these are important in prompting experimental validation of chiral symmetry breaking.

Many interesting experimental systems have been devised to understand the chemical and physical basis of homochirality. Among the most important is that of Soai et al. where, in these systems, a small initial excess of one enantiomer, itself a catalyst for the reaction, produced an enantiomeric excess of greater than 85% of chiral pyrimidyl alkanol [6, 7, 17 -20]. Progress has been made in understanding the use of chiral surfaces to produce a homochiral product [21, 22]. In another experimental system, Kondepudi et al. demonstrated symmetry breaking during crystallization; they showed that stirring during crystallization leads to both symmetry breaking and, above a certain threshold and at large enough stirring rates, the achievement of total chiral purity, i.e. homochirality [6, 23]. Likewise, grinding of racemic mixtures of R and S crystals to produce a homochiral crystal state from supersaturated solutions was observed by Viedma with sodium chlorate and by Noorduin et al. with amino acids [24, 25]. A mathematical description of chiral symmetry breaking was proposed by Wattis [26]. Similarly, deracemization was observed to be induced by a temperature gradient in a boiling slurry of $NaClO_3$ [24]. Perry et al. employed sublimation showing that a near racemic mixture of serine yielded a sublimate with a highly enriched enantiomer [28].

Of particular interest in understanding the chemical evolution of homochirality is the idea that once one molecule, such as a simple amino acid, exists predominantly in one chiral form, it could then serve as a template for the transmission of homochirality to other molecular structures [28-30]. Nanita and Cooks suggest that homochirogenesis leading to biochirality has three steps: chiral symmetry breaking, chiral enrichment, and chiral transmission. Their experiments demonstrate transmission of homochirality from a homochiral serine octamer to cysteine or other amino acids [28]. Hein et al. described how a low concentration of a chiral amino acid biased the reaction producing amino-oxaoline precursors for RNA nucleotides [31, 32]. Breslow and Cheng demonstrated experimentally that L-amino acids can catalyze the formation of D-glyceraldehyde, a simple three-carbon sugar [33]. These results suggest that generation of a single homochiral structure might be sufficient to initiate a process for homochirogenesis on the early Earth.

As noted by Pross and Pascal, we can only speculate on the actual path to life on Earth and elsewhere but, as an important scientific obligation, we can investigate "the principles that would explain the remarkable transformation of inanimate matter to simple life" [34]. In the present paper, we propose a simple chemical model system that does not exhibit features common to reported models. Mathematical analysis of the "toy" model reveals how a "random" perturbation can trigger chiral symmetry breaking and the amplification of one enantiomeric form. One dominant enantiomeric form could act as a possible template for other critical molecules. We describe important kinetic features of our model to facilitate exploration of experimental validation of our chemical system.

2. Methods

2.1. Description of the model

We explored chemical model system that exhibits spontaneous chiral symmetry breaking from an achiral substrate, X, to generate an enantiomeric excess of R or S forms by interaction with an achiral surface. The mechanistic steps of the model were devised so that the kinetic parameters treated both enantiomers equivalently. This simple model system is, undoubtedly, a particular case which might have operated in a prebiotic environment.

Reaction Step	Rate Constant	
$X + C \rightarrow X_C$	k_0	(1)
$X_C \rightarrow R_C$	k_1	(2)
$X_C \rightarrow S_C$	k_1	(3)
$R_C + R \rightarrow R_C + X$	k_2	(4)
$S_C + S \rightarrow S_C + X$	k_2	(5)
$R_C + S \rightarrow S_C + X$	k_3	(6)
$S_C + R \rightarrow R_C + X$	k_3	(7)
$R_C \rightarrow R + C$	k_4	(8)
$S_C \rightarrow S + C$	k_4	(9)

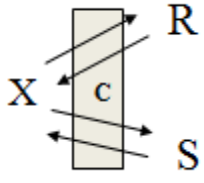

In the model, X represents a prochiral precursor leading to R or S after binding to C, an achiral surface to which X, R or S can bind. The X_C intermediate leads to R_C and S_C, which can either interact with R and/or S, or which can release the chiral products R and S. The critical elementary steps of the mechanism can be described as three sets: in step #1, X binds to C; in steps #2 and #3, X on the achiral surface generates R or S bound to C; in steps #4, #6 and #8, R bound to C is either released or regenerates X after interacting with either R or S. Parallel steps #5, #7 and #9, describe the reactions of S bound to C. Figure 1. depicts these mechanistic steps.

2.2. Computational methods

The model system was explored computationally to search for conditions and regions in kinetic parameter space that resulted in chiral symmetry breaking. Two computational approaches were used: Kintecus 4.50 [35, 36] and Chemical Kinetics Simulator, CKS 1.0, [37]. Kintecus is an Arrhenius-based, chemical simulation program developed by J.C. Ianni that interfaces with Microsoft Excel. It is a deterministic program that solves the governing differential equations of the system. Inputs to Kintecus include the reaction scheme, kinetic parameters (A and E_a), initial concentrations and temperature. Program parameters include selection of the numerical integrator; DASPK, a differential algebraic systems equations solver, was used for all runs. Other program parameters and switches are noted in figure legends. Output includes graphic and numeric information about concentrations of different species over time.

Alternatively, CKS is a program developed by IBM, which uses a stochastic approach to calculate the concentrations of reactants and products over time [37]. This program simulates the collisions between molecules and finds solutions by randomly (i.e. unpredictably) selecting among probability-weighted reaction steps. Like Kintecus, input for CKS includes the reaction scheme, kinetic parameters, initial conditions and temperature. CKS-specific parameters include total number of molecules and a random number seed.

We introduced certain assumptions and initial conditions to simplify the model and to focus on symmetry breaking. The reaction scheme was devised to be symmetrical in processing enantiomers R and S, i.e. reactions #2 and #3 have the same rate constant k_1, etc. To facilitate kinetic and numerical analysis, we assume the mechanistic steps are irreversible.

2.3. Mathematical methods

The governing differential equations that define the system dynamics (see Eq. 10) are non-linear and thus resistant to exact solution. However, they do admit to a stability analysis of the quasi-equilibrium state [38]. In the case where this state is unstable, we are also able to predict the long term (steady state) concentrations of the enantiomers R and S - and the corresponding enantiomeric excess - that result from amplification of the perturbation that triggers the symmetry breaking.

3. Results and discussion

3.1. Computational studies

Kinetic parameters were varied to explore scenarios in which symmetry breaking occurred. In the following examples, we used the representative parameters shown in Table 1. We describe here two initial states: Initial State 1: R = S = 0.0M, X = 1M C = 1 M (held constant) and all intermediates are 0.0M; Initial State 2: R=S=0.5M, X= $1x10^{-6}$M (Note, X=0.0M results in no reaction), C = 1.0M (held constant) and all intermediates are 0.0M.

3.1.1. Initial State 1: X = 1M, R = S = 0M, C = 1 M (held constant)

The results from both Kintecus and CKS, for a temperature of T = 300K, are illustrated in Fig. 2 and 3. The concentrations of R and S rapidly increase to a quasi-equilibrium state, which, after some time (depending on the size of the numerical "trigger" that breaks the symmetry between R and S), bifurcates

to produce a final steady state that represents a mixture with one of the two enantiomers substantially in excess. At this temperature, we obtain an enantiomeric excess, ee = |(R-S)|/(R+S), of 88.1%.

CKS used the same kinetic parameters and initial conditions as Kintecus and used CKS-specific parameters of 100,000 molecules and a random number seed. The enantiomer that was generated in excess varied with input of the random seed, an input feature of the stochastic program. The output from CKS was qualitatively similar to that from Kintecus; both programs showed a quasi-equilibrium state before bifurcation of the concentration curves leading to a steady state with an excess of one enantiomer. Typically, CKS predicted a shorter period in the quasi-equilibrium state.

The differences between the results from CKS and Kintecus were attributed to different methods of numerical analysis but, in both cases, a very small perturbation in the concentration of R or S in the quasi-equilibrium state led to symmetry breaking. In the CKS program, the stochastic nature of the process led to very early symmetry breaking. In Kintecus, the trigger for the chiral symmetry breaking was small round-off errors in the integration algorithm. In these cases, the symmetry breaking leading to an enantiomeric excess randomly favored either chiral form. The large-scale behavior of the system was predictable if a bias was introduced initially; for example, an initial concentration of R = $1x10^{-18}$M with S = 0.0M, predictably lead to an ee of the R isomer (not shown). It is reasonable to propose that these computational perturbations mimic imbalances that could occur in nature.

To investigate the effect of different temperature conditions on the outcomes from Initial State 1, the Kintecus program was run for temperatures in the range from 250K to 500K; the results are shown in Figure 4 and Table 2. As noted in Figure 4 and Table 2, chiral symmetry breaking does not occur above 417K and, below 417K, both the enantiomeric excess and the concentration of the dominant enantiomer increase with decreasing temperature, reaching 90% below T=294K. Note that the enantiomer which dominates in the steady state appears to be random.

Identical final results were obtained if the initial concentration of C was 1.0M and was not held constant. Graphs showed that 1.0M C was in considerable excess (not shown).

3.1.2. Initial State 2: X = 1x10^{-6}M, R=S=0.5M, C=1.0M (constant)

Starting with a racemic mixture of R and S, no reaction occurred if the initial concentration of X was 0.0M, since none of the intermediates, X_C, R_C or S_C could form. With a small initial concentration of X, both Kintecus and CKS predict symmetry breaking from the initial racemic mixture. As shown in Figure 5 for 300K, concentrations of R and S dropped to a quasi-equilibrium state and then, as for the previous case, the concentration plots bifurcate. Curiously, the numerical investigations reveal that the quasi-equilibrium and steady state response of the system are independent of the initial concentrations of all the species, and are wholly determined by the sum of those concentrations, viz: $R+S+X+X_C+R_C+S_C$.

3.2. Mathematical analysis of the model

The governing differential equations that define the system dynamics are non-linear and thus resistant to exact solution. However, they do admit to a stability analysis of the quasi-equilibrium state [26]. In the case where this state is unstable, we are also able to predict the long term (steady state) concentrations of the enantiomers R and S - and the corresponding enantiomeric excess - that results from amplification of the perturbation that triggers the symmetry breaking.

For the kinetic parameters in Table 1, the simulations show that above some temperature (417K for the present system parameters, Fig.1) the quasi-equilibrium state is stable, i.e. no chiral symmetry breaking, but that at lower temperatures, symmetry breaking occurs with amplification leading to a large excess of one enantiomer.

To theoretically investigate the stability of the system, we define a vector in state space, $\underline{Z} = (Z_1, Z_2, Z_3\ldots, Z_6) = (X, X_C, R, S, R_C, S_C)$, where the symbols represent the respective molar concentrations. The governing equations of the chemical system become $dZ_i/dt = f_i(\underline{Z})$, i=1,2,…,6, where the functions f_i are, respectively:

$$
\left.
\begin{aligned}
f_1 &= -k_1XC + k_2(RR_C+SS_C)+k_3(RS_C+SR_C) \\
f_2 &= -2k_1X_C + k_1XC \\
f_3 &= -k_2RR_C - k_3RS_C + k_4R_C \\
f_4 &= -k_2SS_C - k_3SR_C + k_4S_C \\
f_5 &= k_1X_C + k_3(RS_C - SR_C) - k_4R_C \\
f_6 &= k_1X_C + k_3(SR_C - RS_C) - k_4S_C
\end{aligned}
\right\} \qquad (10)
$$

Note, here we consider the case for constant C, but it turns out that the results of the analysis also apply when C is not held constant (C = C(t)).

Since $f_1 + \ldots + f_6 = 0$, it follows that the sum of the time dependent concentrations, i.e. $F=R+S+R_C+S_C+X+X_C$, is itself constant and equal to the sum of the initial concentrations of all chemical species involved (except C). Note that for the present system, the initial conditions are chosen such that F=1. When the system is in its quasi-equilibrium state, we have R = S and $R_C = S_C$. Thus, it is convenient to define – and work with - variables $x_\pm = R \pm S$ and $y_\pm = R_C \pm S_C$ so that the equations $dR/dt = f_3$ and $dS/dt = f_4$ are combined to yield:

$$
\left.
\begin{aligned}
dx_+/dt = g_3 &= -(k_2+k_3)x_+y_+/2 +(k_3-k_2)x_-y_-/2 + k_4y_+ \\
dx_-/dt = g_4 &= -(k_2+k_3)x_-y_+/2 + (k_3-k_2)x_+y_-/2 + k_4y_-
\end{aligned}
\right\} \qquad (11)
$$

and f_5 and f_6 are similarly combined to give

$$
\left.
\begin{aligned}
dy_+/dt = g_5 &= 2k_1X_c - k_4y_+ \\
dy_-/dt = g_6 &= k_3(x_-y_+ - x_+y_-) - k_4y_-
\end{aligned}
\right\} \qquad (12)
$$

In terms of the new variables, the quasi-equilibrium state now becomes:

$$\underline{Z} = (X, X_c, x_+, x_-, y_+, y_-) \sim (X, X_C, 2R, 0, 2R_C, 0).$$

To obtain the criteria for which the state loses stability, we use the method of Lyapunov [26]. First, we perturb the governing equations about the state $\underline{Z}$, viz:

$$d\delta Z_i/dt = \sum_j(\partial g_i(\underline{Z})/\partial Z_j)\delta Z_j = \lambda \delta Z_i \qquad (13)$$

(Note: $g_1 = f_1$ and $g_2 = f_2$) in which λ is the Lyapunov exponent. Determination of the λ's requires solution of the determinental equation:

$$\det \; |\partial g_i(\underline{Z})/\partial Z_j) - \lambda\delta_{ij} | = 0 \qquad (14)$$

in which $\delta_{ij} = 1$ for i=j and 0 for i≠j. That is λ is subtracted from each diagonal term in the determinant, which, for the system in question, is the determinant of a 6 x 6 matrix, resulting in a polynomial of order 6 in λ. For stability of the state, $\underline{Z}$, we require all λ's to be ≤ 0 (and any complex λ's should have real part ≤0.) Some algebra results in the following two requirements for stability:

$$R_C [k_4 (k_2 – k_3) + 4k_2k_3R] > 0, \qquad (15)$$

$$R_C [(2k_1 + k_4)C + 2k_4] + 2k_1[k_4/(k_2+k_3) – R]C > 0 \qquad (16)$$

in which R = S and $R_C = S_C$ are the values at the quasi-equilibrium state.

Numerical analysis of the governing equations, reaction #1-#9, indicates that for $k_4/(k_2+k_3) > F/2$, the quasi-equilibrium state is characterized by R = S = F/2 and $R_c \sim 0$. Thus, condition (16) is automatically satisfied and because R_C~0, the condition (15) is rendered moot, i.e. the quasi-equilibrium state is stable regardless of the value of k_2/k_3.

For $k_4 / (k_2 + k_3) < F/2$, numerical analysis shows that at the quasi-equilibrium state R = S = $k_4/(k_2+k_3)$ so that condition (16) is again automatically satisfied. However, in this case, it is found that R_c and S_c are no longer small in the quasi-equilibrium state, so that $[k_4 (k_2 – k_3) + 4k_2k_3R] > 0$ also needs to be satisfied, viz: $k_4(k_3-k_2) < 4k_2k_3R = 4k_2k_3k_4/(k_2+k_3)$, or equivalently

$$(k_2/k_3)^2 + 4(k_2/k_3) – 1 > 0, \qquad (17)$$

that is $(k_2/k_3) > \sqrt{5} – 2 = 0.236$.

In summary, for $k_4/(k_2+k_3) > F/2$, the quasi-equilibrium state turns out to be stable regardless of the k_2/k_3 ratio: there is no chiral symmetry breaking, but rather the steady state consists of R = S = F/2 = ½. However, for $k_4/(k_2+k_3) < F/2$, we have the two sub-cases, namely i) $k_2/k_3 > \sqrt{5} – 2 = 0.236$ for which the state is stable (no chiral symmetry breaking), with R = S = $k_4/(k_2+k_3)$ and ii) $k_2/k_3 < 0.236$ for which the quasi-equilibrium state bifurcates, that is we have chiral symmetry breaking, to yield a steady state

with $R \neq S$. In this case, the degree of symmetry breaking (dominance of one enantiomer over the other) depends on the ratio k_2/k_3: the smaller the ratio the greater the breaking, the greater the value of the enantiomeric excess, $ee = |(R-S)|/(R+S)$. For the present system, the threshold temperature corresponding to $k_2/k_3 = \sqrt{5} - 2$ is 417K, temperatures above which the system is kinetically stable and will not exhibit symmetry breaking.

In addition to the above stability analysis, from which we were able to predict the steady state value of $R = S$ in the region of parameter space corresponding to $k_2/k_3 > 0.236$ (no chiral symmetry breaking), the governing equations also enable us to investigate the variation with temperature of the steady state concentrations where one enantiomer is in excess for $k_2/k_3 < 0.236$. Combining the dx_+/dt and dx_-/dt, Eqs.(11), we obtain a differential equation for

$ee = x_-/x_+$ viz:

$$dee/dt = (k_3/2)(1-k_2/k_3)(1-ee^2)y_- + k_4(x_+y_- - x_-y_+)/x_+^2. \quad (18)$$

This, together with the equation for dy_-/dt (Eq.(12)), yields in the steady state the relation.

$$1 - ee^2 = 2(k_4/k_3)^2/[(1-k_2/k_3)x_+^2] \quad (19)$$

Manipulation of the dx_+/dt and dy_-/dt equations also yields, in the steady state, the relation

$$\{[1/2\ (1+k_2/k_3)x_+ - k_4/k_3](x_+ + k_4/k_3) - \tfrac{1}{2}\ (1-k_2/k_3)x_+^2 ee^2\}y_+ = 0. \quad (20)$$

For $y_+ \neq 0$, combining Eqs. (19) and Eq.(20) yields separate relations for x_+ and ee, viz

$$x_+ = \tfrac{1}{2}\ (k_4/k_3)(1-k_2/k_3)/(k_2/k_3) \quad (21)$$

and $$1-ee^2 = 8(k_2/k_3)^2/(1-k_2/k_3)^3, \quad (22)$$

from which R and S follow immediately, using $(R,S) = (x_+/2)(1\pm ee)$.

Furthermore, solving Eq.(22) for $ee = 0$ yields the aforementioned result $k_2/k_3 = \sqrt{5} - 2$, as expected.

The above analysis of the model is consistent with the results from the simulation summarized in Figures 2-4 and Table 2, using the parameters in Table 1: The threshold $k_2/k_3 = \sqrt{5} - 2$ occurs at T~417K. Thus, for T > 417K, there is no chiral symmetry breaking; rather $R=S=k_4/(k_2+k_3)$. Conversely, for T< 417K, there occurs chiral symmetry breaking with $x_+ = R + S$ and ee both increasing as T decreases, per

the predictions of Eqs. (21) and (22). However, below the temperature corresponding to $x_+ = 1$ (Eq.(21)), the condition $y_+ > 0$ that led to Eqs.(21) and (22) ceases to be valid: we enter a region (not shown in the Table 2 but verified in simulations elsewhere in parameter space) in which X, Xc, Rc and Sc became ~0 and R + S = 1, i.e. the concentration of X was limiting. However, we find that using $x_+ = 1$ in Eq.(19) continues to yield values of ee that are remarkably close to those obtained numerically. Thus, we can now claim with confidence the ability to predict the steady state values of R and S at ALL temperatures directly from the system's governing equations.

3.3. Further exploration of phase space.

The parameters of Table 1, used in the aforementioned simulation, were chosen somewhat arbitrarily. To more completely understand the kinetic behavior of the model, we investigate here the possibility of constraining the space of E_a's. To that end, we first note that the Arrhenius coefficient A and the energy $E_{a0} = E_{a1}$, used to specify the reaction constants $k_o = k_1$, can, at some arbitrary temperature, be used to set the time scale; the value of k_1 is not critical to either the quasi-equilibrium state or the asymptotic steady state of the system. Arbitrarily fixing E_{a2} (yielding k_2), suppose we now *specify/constrain* the temperature $T=T_1$ at which the chiral symmetry breaking threshold $k_2/k_3 = \sqrt{5} - 2$ occurs; then the energy level E_{a3} follows, viz: $E_{a3} = E_{a2} + RT_1\ln(\sqrt{5} - 2)$. Likewise, suppose we also *specify/constrain* the temperature T_2 corresponding to the $R = S = F/2 = ½$ threshold $k_4/(k_2 + k_3) = F/2 = ½$; then, using $(k_4/k_3)/(1 + k_2/k_3) = (k_4/\sqrt{(k_2k_3)})/(\sqrt{(k_2/k_3)} + \sqrt{(k_3/k_2)})$, and substituting $(E_{a3} - E_{a2})/R = T_1\ln(\sqrt{5} - 2)$, E_{a4} follows from $E_{a4} = (E_{a2} + E_{a3})/2 - RT_2\ln\{\cosh[(T_1/(2T_2))\ln(\sqrt{5} - 2)]\}$. For example, starting with $E_{a2} = 15$, imposing $T_1 = 400$K leads to $E_{a3} = 10.2$, and $T_2 = 600$K then leads to $E_{a4} = 12.04$. Alternatively, imposing $T_1 = 300$ and $T_2 = 400$, leads to $E_{a3} = 11.4$ and then $E_{a4} = 12.74$. Curiously, one could choose $T_1 = T_2$, for which the system would just miss out on the region of parameter space corresponding to the steady state ee=0 and R=S < F/2. In this scenario, for $T<T_1$ the ee and $x_+ = R+S$

would increase with decreasing temperature, with R+S=constant=F below a sufficiently low temperature; and, for $T>T_1$ the steady state would be R=S=F/2 independent of temperature.

That is - notwithstanding the arbitrariness in the choice of A and E_{a1} (to determine the time scale t) - by imposing values for the threshold temperatures T_1 and T_2, the number of "degrees of freedom" in parameter space can be effectively reduced to one, namely the choice of E_{a2}.

4. Conclusions

Systems chemistry is an important new discipline that investigates the behavior of interacting chemical reactions [39, 40]. Like systems biology and systems engineering, a critical feature of systems chemistry is that unexpected outcomes may arise which may not be predicted from examining the behavior of the individual components of the system. We have studied, both computationally and analytically, several simple chemical systems and have found that complex behavior can arise over time from even simple systems [41-43]. Recently we and others have focused on chemical systems to understand the generation of homochirality in prebiotic environments.

We demonstrate chiral symmetry breaking in a simple chemical model system in which the dynamic behavior is non-linear and explore the conditions under which small perturbations in symmetry are amplified to near homochirality. While the governing differential equations, being non-linear, are difficult to solve analytically, we have been able to analytically investigate both quasi-equilibrium and steady state behavior, and to thereby predict the conditions under which symmetry breaking results in such enantiomeric enhancement. Such analytical predictions agree with all results of numerical simulation – both deterministic and stochastic - of the chemical system.

The chemical system was designed to treat R and S (as well as R_C and S_C) symmetrically. Conditions were found that resulted, after a meta-stable equilibrium state, in a random but exceeding small numerical perturbation of the state; that perturbation was then amplified to a new steady state in which there was an enantiomeric excess. Others have simulated spontaneous breaking in perfectly autocatalytic symmetrical model systems due to fluctuations or reaction "noise" [10-13, 44, 45]; these

Frank-like systems depended on autocatalytic and mutual inhibitory reactions. Non-linear kinetic behavior is a feature of all these systems.

How might models of chiral symmetry breaking reflect "real" chemistry? A perturbation (or so-called "butterfly effect" [38]) – introduced in a computational model either explicitly as an initial bias or implicitly due to a numerical perturbation in the computation algorithm or introduced in the natural environment by external sources, for example from constituents of meteorites [29, 46, 47] – initiates chiral symmetry breaking; the non-linear system dynamics then cause amplification of one enantiomeric form over the other [8-11, 16, 44, 45]. It is important to note that spontaneous chiral symmetry breaking may not require a chiral environment. For example, Soai and colleagues have shown absolute asymmetric synthesis and enantiomer enrichment using achiral silica gel [48, 49]. Our model suggests that symmetry breaking may occur in simple chemical systems where there is interaction between an achiral monomeric species, such as a prochiral precursor to an amino acid, and an achiral surface.

Our model gives further support to the notion that generation of a key molecule in a predominately chiral form could act as a template for other important structures and thereby provide an environment that would promote synthesis of chiral precursors leading to functioning macromolecules.

Acknowledgements

CB and PMS gratefully acknowledge funding through the Connecticut Space Grant Consortium and the University of New Haven Faculty Research Support. BNM and JMK thank the University for supporting undergraduate summer fellowships and NASA for a CT Space Grant Fellowship (BNM).

References

1. D.G. Blackmond, Cold Spring Harbor perspectives in biology, 2(5), (2010) a002147. doi: 0.1101/cshperspect.a002147

2. J.D. Carroll, Chirality, 21, 354–358, (2009)

3. M. Wu, S.I. Walker and P. G. Higgs, Astrobiology, 12, 818-829 (2012)

4. M. Gleiser and S. I. Walker, arXiv preprint arXiv, 1202.5048 (2012)

5. F.C. Frank, Biochim. Biophys. Acta, 11, 459-463 (1953)

6. P. V. Coveney, J. B. Swadling, J. A. Wattis and H.C. Greenwell, H. C., Chem. Soc. Rev., 41, 5430-5446 (2012)

7. M. Klussmann, Genesis-In The Beginning, 22, 491-508 (2012)

8. B. Barabás, J. Tóth and G. Pályi, J. Math. Chem., 48, 457–489 (2010)

9. D. Lavabre, J-C. Micheau, J.R. Islas and T. Buhse, Top. Curr. Chem., 284, 67–96 **(**2008)

10. D. Hochberg and M-P. Zorzano. Chem. Phys. Lett., 431, 185-189 (2006)

11. V. S. Gayathri and M. Rao, Europhysics Letters, , 80, 28001 (2007) doi:10.1209/0295-5075/80/28001

12. D. Todorovi, I. Gutman and M. Radulovic, Chem. Phys. Lett., 372, 464–468 (2003)

13. M. Mauksch and S.B. Tsogoeva, Chem Phys Chem., 9, 2359 – 2371 (2008)

14. Y. Saito and H. Hyuga, Top. Curr. Chem., 284, 97-118 (2008)

15. R. Plasson, H. Bersini and A. Commeyras, Proc. Natl. Acad. Sci. USA, 101, 16733-16738 (2004).

16. M. Gleiser, B.J. Nelson and S.I. Walker, Orig. Life Evol. Biosph., 42, 333–346,(2012)

17. K. Soai, T. Shibata, H. Morioka and K. Choji, K., Nature, 378, 767-768, (1995)

18. M. Maioli, K. Micskei, L. Caglioti,C. Zucchi and G. Pályi, J. Math. Chem., 43(4), 1505-1515 (2008)

19. K. Micskei, G. Rábai, E.Gál, L. Caglioti and G. Pályi, J. Phys. Chem. B,112, 9196-9200. (2008).

20. L. Caglioti and G. Pályi, Rend. Fis. Acc. Lincei, 24, 191-196 (2013).

21. P.C. Joshi, M.F. Aldersley and J. P. Ferris, Adv. Space Res., (2012), http://dx.doi.org/10.1016/j.asr.2012.09.036

22. P.C. Joshi, M.F. Aldersley and J.P. Ferris, Orig. Life Evol. Biosph., 41, 213-236 (2011)

23. D. K. Kondepudi and K. Asakura, Acc. Chem. Res., 34, 946-954 (2001)

24. C. Viedma and P.Cintas, Chem. Commun., 47, 12786–12788 (2011)

25. W. L. Noorduin, T. Izumi, A. Millemaggi, M. Leeman, H. Meekes, W.J.P. Van Enckevort, R. M. Kellogg, B. Kaptein, E. Vlieg and D. G. Blackmond, J. Amer. Chem. Soc., 130(4), 1158-1159 (2008)

26. J.A. Wattis, Orig. Life Evol. Biosph., 41, 133-173 (2011)

27. R.H. Perry, C. Wu, M. Nefliu and R. G. Cooks, 10, 1071–1073 (2007)

28. S.C. Nanita and R.G. Cooks, Angew Chem Int Ed Engl., 45, 554-569 (2006)

29. A.L. Weber and S. Pizzarello, Proc. Natl. Acad. Sci. USA, 103, 12713-12717 (2006)

30. A. L. Caglioti, K. Micskei and G. Pályi, Chirality, 23.1, 65-68 (2011)

31. J.E. Hein, E. Tse and D.G. Blackmond, D. G., Nature Chemistry, 3, 704-706 (2011)

32. J.E. Hein and D.G. Blackmond, Acc. Chem. Res., 45, 2045-54 (2012)

33. R. Breslow and Z.L. Cheng, Proc. Natl. Acad. Sci. USA, 107, 5723-5725 (2010)

34. B. A. Pross, R. Pascal, Open Biol., 3, 120190 (2013)

35. J.C. Ianni, Kintecus , Windows Version 4.01, (2010) Available online at: http://www.kintecus.com and Kintecus Manual: http://www.kintecus.com/Kintecus_V400.pdf Accessed 25 June 2013

36. J.C. Ianni, Computational Fluid and Solid Mechanics, 2003, 1368–1372 (2003)

37. W.D. Hinsberg and F.A. Houle, Chemical Kinetics Simulator, v1.01, IBM, Almaden Research Center, (1996). Available online at: www.almaden.ibm.com/st/msim Accessed 25 June 2013

38. S.H. Strogatz, Nonlinear Dynamics and Chaos with Applications to Physics, Chemistry and Engineering (Perseus Books, Reading, MA. 1994), pp. 123-138.

39. R. F. Ludlow and S. Otto, Chem. Soc. Rev., 37, 101-108 (2008)

40. M. Kindermann, I. Stahl, M. Reimold, W. M. Pankau and G. von Kiedrowski, Angew Chem Int Ed Engl., 44, 6750-6755 (2005)

41. P.M. Schwartz, D.M. Lepore and C. Barratt, International Journal of Chemistry, 4, 9-15 (2012)

42. D.M. Lepore, C. Barratt and P.M. Schwartz, J. Math. Chem., 49, 356-370 (2011)

43. D.C. Osipovitch, C. Barratt and P.M. Schwartz, New J. Chem., 33, 2022-2027 (2009)

44. J. R. Islas, D. Lavabre, J-M. Grevy, R. H. Lamoneda, H. R. Cabrera, J-C Micheau and T. Buhse, Proc. Natl Acad. Sci., USA, 102, 13743–13748 (2005)

45. M. Mauksch and S.B. Tsogoeva, Biomimetic Organic Synthesis, 23, 823-845 (2011) doi: 10.1002/9783527634606.ch23

46. M.H. Engel and S. A. Macko, Precambrian Research, 106, 35-45 (2001)

47. S. Pizzarello, Acc. Chem. Res., 39, 231 – 235 (2006).

48. T. Kawasaki, K. Suzuki, M. Shimizu, K. Ishikawa and K. Soai, Chirality, 18, 479–482 (2006)

49. T. Kawasaki and K. Soai, J. Fluorine Chem., 131, 525–534 (2010)

Table 1. Kinetic Parameters

Rate Constants	Arrhenius Constant (A)	Energy of Activation (E_a)
k_o	1.00×10^3	30
k_1	1.00×10^3	30
k_2	1.00×10^3	15
k_3	1.00×10^3	10
k_4	1.00×10^3	14

Table 2. Effect of temperature on chiral symmetry breaking

Temperature (K)	$k_4/(k_2+k_3)$	k_2/k_3	CONC. (R=S) at Quasi-equil.	Final CONC. R	Final CONC. S	SUM [R] + [S]	Enantiomeric Excess
250	0.1339	0.0902	0.1339	0.7190	0.0163	0.7353	95.6%
275	0.1563	0.1122	0.1563	0.0257	0.6620	0.6877	92.5%
300	0.1773	0.1347	0.1773	0.6080	0.0385	0.6465	88.1%
325	0.1970	0.1571	0.1970	0.0554	0.5550	0.6104	81.9%
350	0.2150	0.1794	0.2150	0.0779	0.5010	0.5789	73.1%
375	0.2310	0.2012	0.2310	0.1090	0.4420	0.5510	60.4%
400	0.2460	0.2225	0.2460	0.3670	0.1580	0.5250	39.7%
415	0.2540	0.2347	0.2540	0.2890	0.2230	0.5120	12.9%
417	0.2551	0.2365	--	0.2551	0.2551	0.5102	0.0%
425	0.2594	0.2430	--	0.2594	0.2594	0.5188	0.0%
450	0.2719	0.2628	--	0.2719	0.2719	0.5438	0.0%
500	0.2938	0.3003	--	0.2938	0.2938	0.5876	0.0%

Rate constants at different temperatures are calculated from the Arrhenius equation, $k = A\, e^{-Ea/RT}$ in which R is the universal gas constant, 8.314×10^{-3} kJ/(K · mol). Concentrations were outcomes from the Kintecus. Enantiomeric excess was determined using the final concentrations: |[R] – [S]| / [R] + [S]. The colored values of [R] or [S] indicates the enantiomer formed in excess

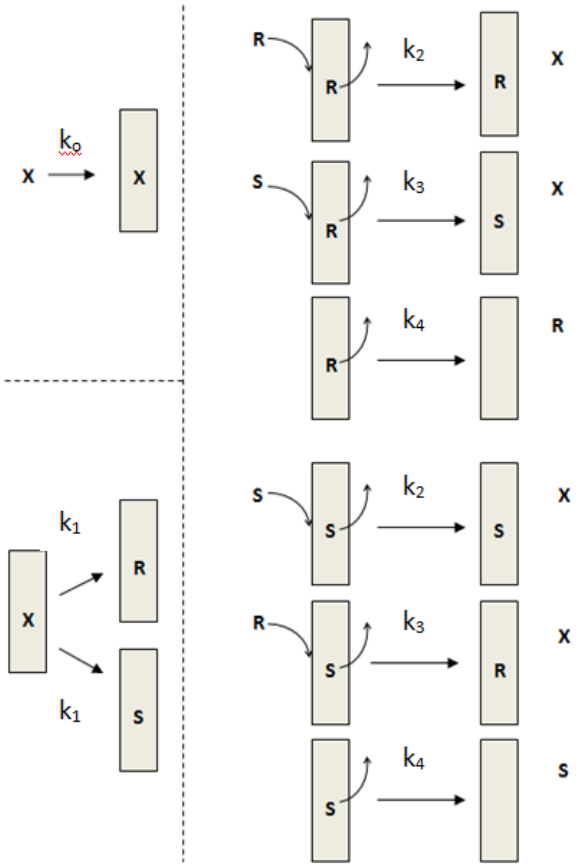

Fig. 1. Mechanistic steps describing the chemical model system – reaction #1-#9

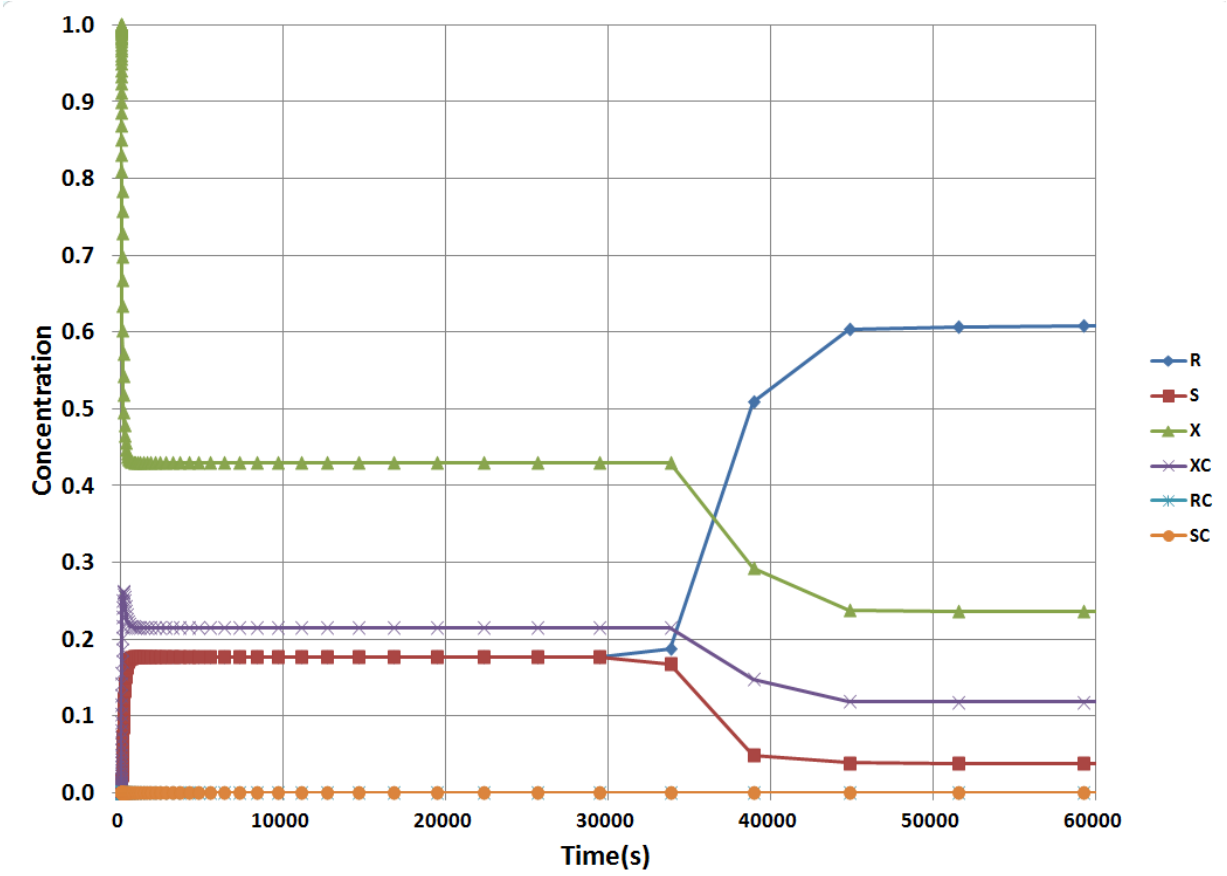

Fig. 2. Output from deterministic analysis of model at 300K. Initial State 1: X = 1M, R = S = 0M, C = 1 M (held constant). Input: Reactions #1-#9; Kinetic parameters: Table 1; Kintecus switches: -ig:mass; starting integration time and maximum integration time, $1x10^{-2}$ sec; accuracy, $1x10^{-13}$

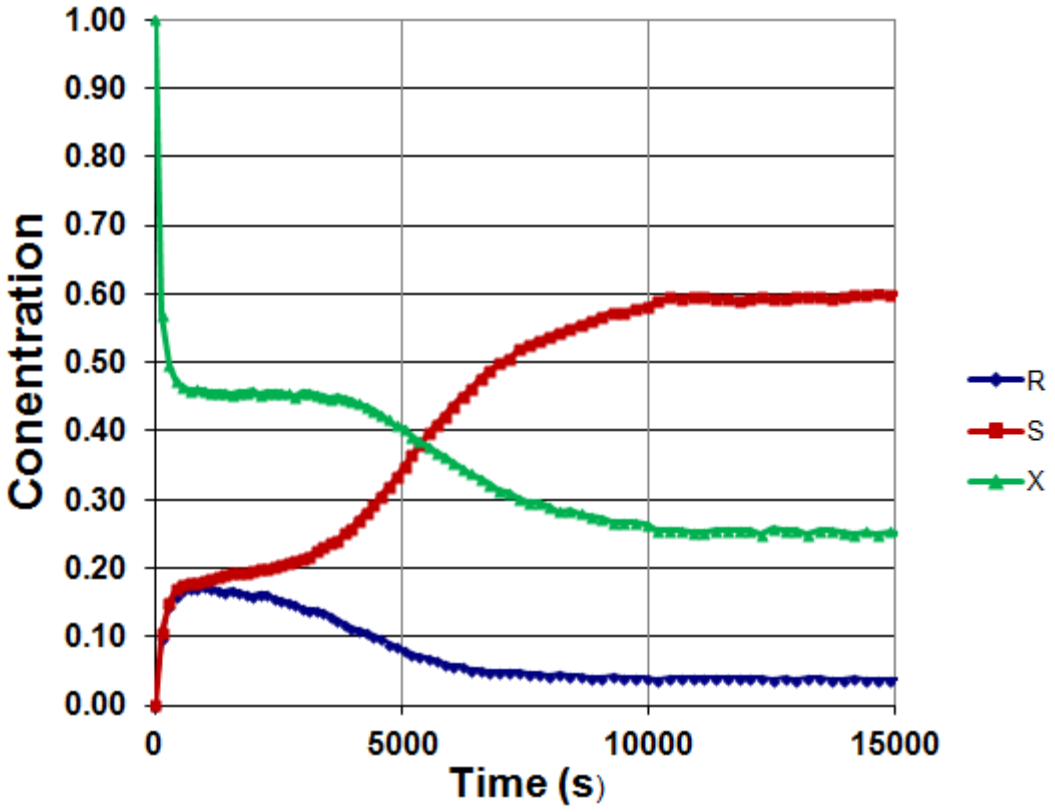

Fig 3. Output from stochastic analysis of model at 300K. Initial State 1: X = 1M, R = S = 0M, C = 1 M (held constant). Input: Reactions #1-#9; CKS Parameter: 100,000 total molecules

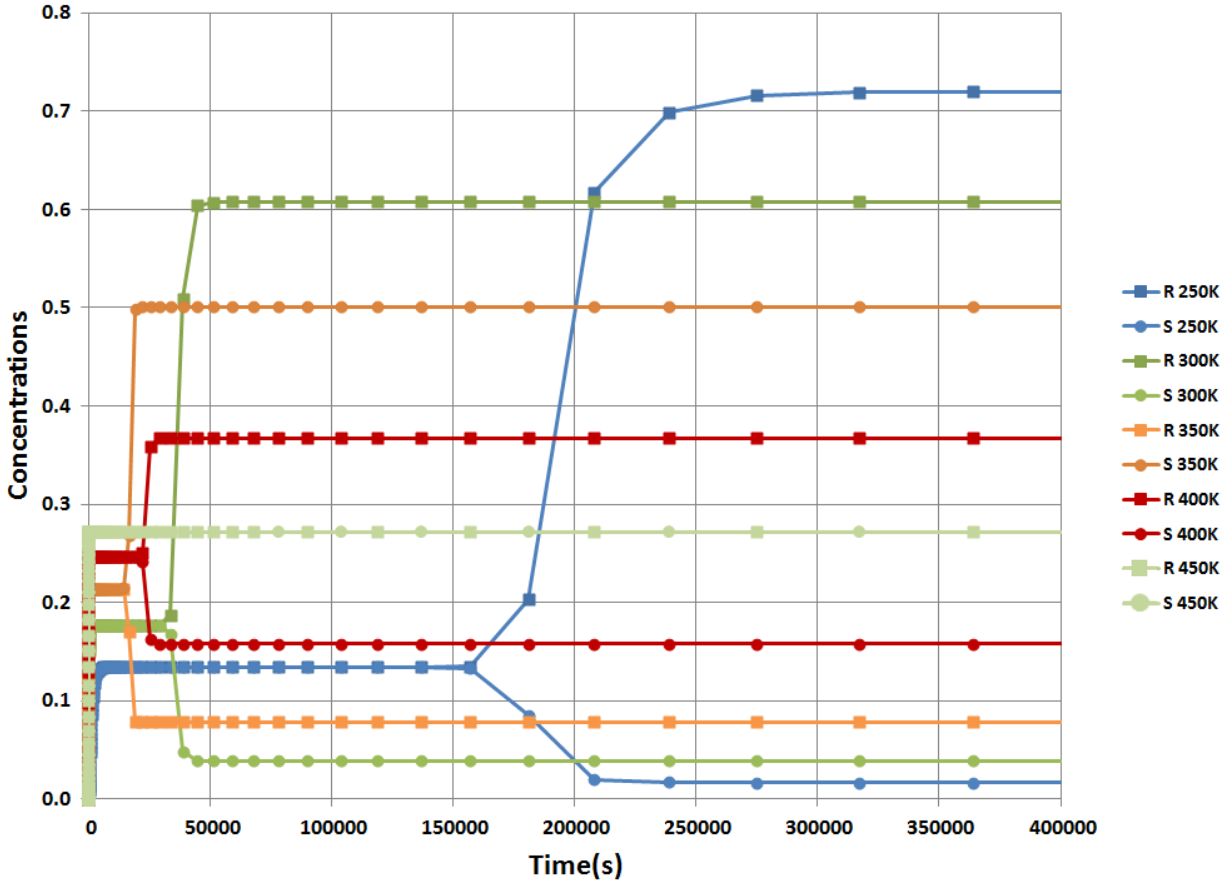

Fig. 4. Output from deterministic analysis of model for enantiomers R (−■−) and S (−●−) at different temperatures. Initial State 1: X = 1M, R = S = 0M, C = 1 M (held constant). Input: Reactions #1-#9; Kinetic parameters: Table 1. Kintecus switches: -ig:mass; starting integration time and maximum integration time, $1x10^{-2}$ sec; accuracy, $1x10^{-13}$

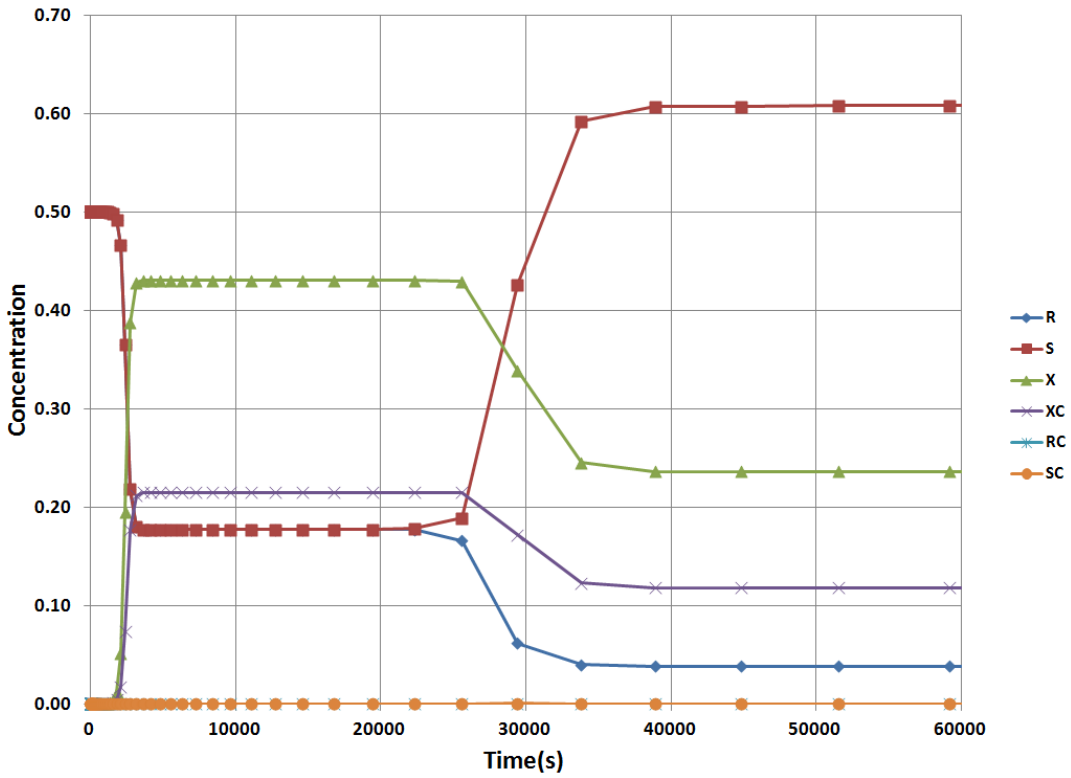

Fig. 5. Output from deterministic analysis of model at 300K. Initial State 2: X = $1x10^{-6}$M, R=S=0.5M, C=1.0M (constant) Input: Reactions #1-#9; Kinetic parameters: Table 1; Kintecus switches: -ig:mass; starting integration time and maximum integration time, $1x10^{-2}$ sec; accuracy, $1x10^{-13}$